Resources, Conservation & Recycling 224 (2026) 108561

Contents lists available at ScienceDirect

Resources, Conservation & Recycling

journal homepage: www.sciencedirect.com/journal/resources-conservation-and-recycling

Full length article

A knowledge based method for estimating the material content value of end of life PCBs

Paolo Citterio *, Francesco Baiguera, Marcello Colledani

Politecnico di Milano, Department of Mechanical Engineering, Technology and Production Systems Lab, Via La Masa 1, 20156, Milan, Italy

ARTICLE INFO

Keywords:
PCBs recycling
Waste PCBs
Precious metals
PCBs sorting
Classification

ABSTRACT

End-of-life printed circuit boards (PCBs) are a high-value but complex waste stream, particularly for small and medium-sized enterprises (SMEs) that lack access to cost-effective recovery technologies. Manual sorting remains the industry norm, hindered by the absence of scalable, automated tools for real-time characterization. This limits material recovery and reduces profitability.

This study introduces a novel, knowledge-based method for PCB characterization that estimates the recoverable value of gold, silver, and copper, metals which account for approximately 90 % of a PCB's total material value, based on the number, size, and geometric features of surface-mounted components. While individual metal content estimations show a mean absolute percentage error of 23.3 %, the method correctly predicted the grade classification of all but one PCB types in a representative validation sample.

This is the first approach to enable low-cost, inline estimation of PCB material grade using component-level visual analysis. By supporting automated, value-based sorting, the method offers a practical and scalable solution for SME recyclers, improving both economic viability and material recovery in electronic waste management.

1. Introduction

The rapid proliferation of electronic devices has led to a significant increase in electronic waste (e-waste), with printed circuit boards (PCBs) representing a substantial fraction of this waste stream. PCBs contain valuable materials such as gold (Au), silver (Ag), copper (Cu), palladium (Pd), platinum (Pt), rare earth elements, and ceramics.

This paper introduces a novel, knowledge-based method for predicting the recoverable value of PCBs through visual and geometric analysis of mounted electronic components. Unlike current approaches, which rely on laboratory techniques or subjective manual sorting, our method enables fast, cost-effective, and automated estimation of Gold, Silver and Copper content, which account for around 90 % of a PCB's material value. The tool is designed specifically to support small and medium-sized recycling enterprises (SMEs) in value-based classification and sorting.

Despite the high intrinsic value of PCBs, material recovery remains inefficient, particularly for SMEs, which represent over 90 % of recycling companies in Europe. These recyclers often lack access to cost-effective technologies and therefore rely on manual classification by trained operators. This process is slow, error-prone, and unscalable, limiting profitability and recovery efficiency.

Parallel to economic consideration, the management and recycling of printed circuit boards (PCBs) are increasingly shaped by regulatory frameworks aimed at reducing environmental harm and promoting resource recovery. The Basel Convention plays a central role by controlling the transboundary movement of hazardous electronic waste, including PCB-containing materials, and recently expanded to include stricter controls on mixed e-waste streams. In the European Union, directives such as WEEE (2012/19/EU) and RoHS (2011/65/EU) enforce mandatory collection, treatment, and restrictions on hazardous substances in electronics to enhance recyclability and reduce pollution. China and other major economies have also implemented national regulations that require licensing, safe dismantling practices, and investment in recycling infrastructure. Despite these efforts, disparities in enforcement, informal recycling markets, and a lack of standardized classification systems remain global challenges.

Existing material analysis techniques are often laboratory-based and resource-intensive, making them unsuitable for SME applications. The issue is not limited to Europe; Goleva et al. (Goleva et al., 2019) provide

* Corresponding author.
E-mail address: paolo1.citterio@polimi.it (P. Citterio).

https://doi.org/10.1016/j.resconrec.2025.108561
Received 10 April 2025; Received in revised form 28 June 2025; Accepted 16 August 2025
Available online 27 August 2025

an overview of material flows and metal recovery from waste PCBs in Australia, showing that a large proportion of PCBs are either landfilled, partially dismantled without recovery, or exported for reuse or disassembly, highlighting a broader global inefficiency in e-waste processing.

Additionally, post-consumer PCBs are a highly heterogeneous product class in terms of size, shape, and material composition. Limited data are available on the elemental content of specific PCB components, even though key metals are often concentrated in certain packages. Early-stage knowledge of a PCB's material value would significantly assist recyclers in selecting the most appropriate end-of-life strategy.

Our method leverages a structured classification of electronic components based on their geometric and functional attributes, linking them to typical material compositions. A supporting algorithm and software tool process input data derived from PCB visual analysis to estimate material value. This enables automated, inline classification and sorting, improving decision-making and profitability in electronic waste treatment—particularly for SMEs with limited resources.

The remainder of this paper is structured as follows: Section 2 reviews the state of the art in PCB characterization and composition analysis. Section 3 presents the proposed knowledge-based classification method. Sections 3.1 and 3.2 provide detailed examples of the material estimation models. Section 4 validates the method through experimental testing. Conclusions are presented in Section 5.

2. PCB recycling and characterization methods: A brief review

The recycling of printed circuit boards (PCBs) is particularly challenging due to their heterogeneous composition, which includes multiple materials and multilayer structures. The increasing miniaturization of electronic devices further complicates material recovery and recycling. As demand for raw materials and energy for integrated circuits (ICs) and electronic components remains high, recycling plays a crucial role in mitigating resource depletion and reducing environmental impact (A. Canal Marques et al. (Marques et al., 2013), R. Vetri Murugan et al. (Vetri Murugan et al., 2008)). The significant energy consumption required for primary material extraction has become a key driver for recovering copper and precious metals from electronic waste. Copper recovery from Waste Electrical and Electronic Equipment (WEEE in the following) is not only economically valuable but also reduces the environmental impact associated with primary copper mining and ore extraction (A. Canal Marques et al. (Lee et al., 2012; Marques et al., 2013)). The economic potential of WPCB recycling is significant. For example, in a medium-sized Brazilian city, an estimated 149.9 tons of WPCBs could be collected annually, with recoverable materials valued at over USD 255,000—representing approximately 3.24 % (de Carvalho et al., February 2025)of the city's annual urban cleaning costs. This demonstrates that material recovery from WPCBs can directly support local waste management systems, strengthening the case for investments in reverse logistics and recycling infrastructure.

A fundamental aspect of efficient recycling is the detailed analysis of PCB material composition. Wang et al. (Wang and Gaustad, 2012) demonstrated that recovery priorities depend on the specific composition of PCBs, with direct implications for both environmental and economic outcomes. PCBs found within WEEE typically consist of a mix of high- and low-grade boards. However, recyclers often lack the automated identification and sorting technologies necessary to separate them effectively. When PCBs are shredded indiscriminately along with the WEEE stream, a substantial share of valuable metals becomes diluted or lost. In contrast, disassembling PCBs prior to processing allows for classification based on material value, thereby enabling optimized handling and improved recovery rates (D. Guarde et al. (Guarde et al., 2014)).

Currently, compositional characterization is typically performed using destructive, lab-based techniques such as Inductively Coupled Plasma Optical Emission Spectrometry (ICP-OES) and Scanning Electron Microscopy (SEM) with Energy Dispersive Spectroscopy (EDS). These techniques, although accurate, are expensive, time-consuming, and unsuitable for real-time or in-line classification prior to recycling. The structural complexity of PCBs, as described by J. Cui et al. (Cui and Forssberg, 2003), often requires several recycling steps to achieve efficient material recovery. M. Colledani et al. (Colledani et al., 2014; Tolio et al., 2017) emphasized that successful demanufacturing strategies depend on integrating multiple technologies alongside optimized management systems and business models. After mechanical size reduction, PCBs are processed through various physical separation methods, including gravity, magnetic, electrostatic separation, and froth flotation (M. Kaya (Kaya, 2016)). These are frequently followed by hydrometallurgical extraction methods. For example, Y. J. Park (Park and Fray, 2009) employed a multi-step process involving shredding, magnetic separation, and eddy current separation, followed by leaching with hexafluorotitanic acid (HBF_4) and ammonium sulfate ($(NH_4)_2SO_4$) to extract solder and copper, and concluded with electrowinning for final metal recovery.

Component composition also significantly influences recovery strategies. For example, tantalum is primarily found in capacitors (J. Li et al. (Li et al., 2004)), while ceramic materials such as aluminum oxide (Al_2O_3) and zinc oxide (ZnO) are present in resistors and ceramic capacitors. Electrolytic capacitors contain considerable amounts of aluminum in their casings and internal foils. The highest concentrations of precious metals are typically found in surface-mounted devices (SMDs) and integrated circuits (ICs), which contain gold, gallium, silicon, selenium, and germanium in varying proportions (J. Li et al. (Li et al., 2004)). Industry leaders such as Umicore have established gold-content-based classification systems (in ppm), see Table 1, which are widely adopted for PCB sorting. An alternative categorization was proposed by T. Havlik et al. (Havlik et al., 2014), who classified PCBs according to application categories—such as consumer electronics, IT and telecommunications, small household appliances, and large household appliances. However, variations in metal content across these categories complicate sorting and recovery.

Powder characterization following shredding has also been explored. M. Delfini et al. (Delfini et al., 2011) analyzed 21 tons of WEEE, identifying that PCBs made up about 5 % of the total weight. They found that IT PCBs contained 96 % of the total gold content, with ICs and processors averaging 2400 ppm of gold. These components constituted around 13 % of the PCB weight, resulting in an overall gold concentration of 312 ppm. Additionally, palladium was detected in varistors, ceramic capacitors, and multilayer ceramic capacitors (MLCCs). A. C. Kasper et al. (Kasper et al., 2011) investigated copper characterization in mobile phone PCBs and demonstrated that mechanical pre-treatment effectively separates metal-rich fractions. Their process used aqua regia dissolution and electrowinning for copper recovery, with SEM/EDS confirming high purity. Similarly, L. H. Yamane et al. (Yamane et al., 2011) found that mobile phone PCBs had a higher copper content (34.5 %) than IT PCBs (20 %), indicating that copper recovery is more feasible for mobile phone recycling, while IT PCBs are more suitable for precious metal extraction.

Emerging technologies based on computer vision and artificial intelligence (AI) offer promising approaches for PCB classification and material recognition. Seungsoo Park et al. (Park et al., 2018) developed an image analysis algorithm using a pixel-based identification technique

Table 1
PCBs classification according to Umicore (http://www.unicore.com).

PCBs	*Gold content*
Very high grade	>400 ppm
High grade	>200 ppm
Medium grade	>100 ppm
Low grade	>50 ppm
Very low grade	<50 ppm

to assess copper liberation in shredded PCBs. Kleber et al. (Kleber et al., 2014; Pramerdorfer and Kampel, 2015) explored laser-induced breakdown spectroscopy (LIBS) for rapid chemical analysis and classification of PCBs and their components. Charpentier et al. (Charpentier et al., 2024) presented new separation and recovery techniques that improve the extraction of gold, copper, and palladium while minimizing the generation of hazardous waste, underlining the potential of integrating advanced technologies into current frameworks to improve both economic feasibility and environmental sustainability.

More recently, Himanshu Sharma and Harish Kumar (de Carvalho et al., February 2025) proposed a computer vision algorithm capable of detecting integrated circuits in real time. This recognition model could eventually be applied in recycling facilities to identify ICs automatically, enhancing material recovery and reducing the volume of valuable components sent to incineration or landfilling. Similarly, Iftikhar A. Soomro et al. (Soomro et al., February 2022) developed a classification system using deep learning to identify PCB types (e.g., RAM, motherboard) in-line.

Despite these advancements in automated recognition, a scalable, cost-effective, and fully automated PCB sorting system remains an open research challenge. Notably, no current image-processing model estimates the precious metal content of PCBs, a critical gap in developing truly effective classification solutions for the recycling industry.

3. Knowledge-based characterization method

The aim of this paper is to demonstrate that the quantity of precious metals—particularly copper, gold, and silver—varies based on the number and type of electronic packages soldered onto the PCB. Once the material content of the PCB is estimated, strategic decisions can be made regarding the treatment process. The proposed knowledge-based characterization method consists of two main steps.

The first step involves developing predictive equations to determine the material content of a PCB based on the geometric and functional properties of its electronic components, substrate, and finishing. Section 3.1 details the method for electronic components and capacitors while Section 3.2 focuses on the finishing and substrate materials. Once established, these models can be applied to any type of PCBs

The second step involves a visual analysis of the specific PCB to obtain the input variables required for the predictive equations developed in the first step. This can be done by an inline operator, or better by an automatic machine, using cameras and a recognition algorithm

This article is focused only on the first step of the process and in the following sections the predictive models are presented.

Fig. 1 below shows how the entire process works.

3.1. Electronic components material composition prediction

The content model used in this work estimates the material composition of PCBs by aggregating the contributions of their individual components. Specifically, the total concentration of a target material is calculated by summing the estimated material quantities of all components mounted on a board, and then normalizing this value by the overall PCB weight. This results in a mass fraction that represents the content of each relevant material per unit of PCB mass.

To estimate the material composition of each component, the model employs predictive equations tailored to specific electronic package types. These equations are analytical functions derived from dimensional and geometric properties, and are designed to output the quantity of each material (e.g., copper, gold, plastic, silicon) contained in the package. The packages considered in this study include Ball Grid Arrays (BGA), Quad Flat Packs (QFP), and Small Outline Integrated Circuits (SOIC), as illustrated in Fig. 2.

Each function relates the physical dimensions of the package (e.g., body size, pin count, thickness) to the expected volume or mass of constituent materials. These relationships have been formulated using data from publicly available material declarations, such as those provided in component datasheets and compliance documents. Given the limited availability of detailed material declarations for every specific package and manufacturer, the model assumes that packages within a defined dimensional range exhibit similar material compositions across brands and product lines. This simplification is supported by the findings of Van Meensel et al. (2014), who showed that such generalizations produce acceptable accuracy in PCB material estimations for recycling applications.

By combining these package-level material content models with the component inventory of a given PCB, the model provides a scalable and systematic approach for estimating the total recoverable material content without requiring destructive testing or exhaustive manual classification.In a symbolic representation, the output of the analytical function can be expressed as a vector, where the components represent the quantities of base (copper) and valuable materials (gold and silver). Mathematically, this can be written as, where T = type of package (dimensions):

$$v1 = [Cu, Au, Ag]T$$

Here, "dimensions" refers to the characteristic 2D dimensions of the

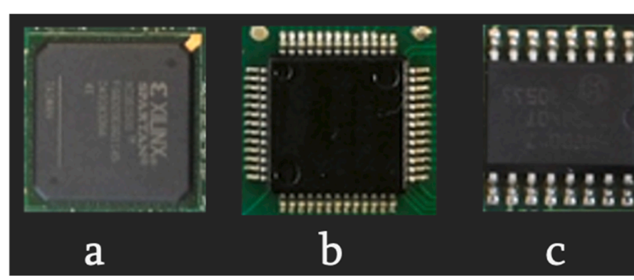

Fig. 2. Packages considered in the analysis: BGA(a) QFP(b).

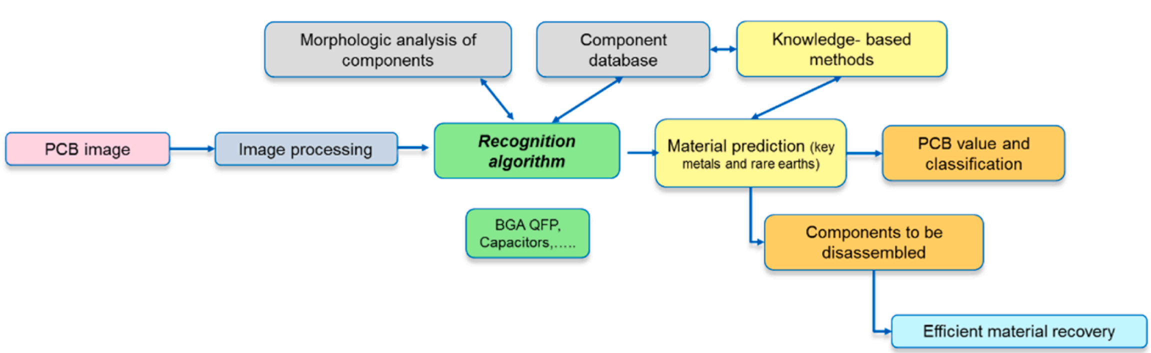

Fig. 1. Outline of the proposed knowledge-based characterization method based on material declarations and visual analysis.

component in the plane. These dimensions account for both the plastic package and metallic terminations. The out-of-plane dimension is neglected, as it has minimal influence on the quantities of the considered metals.

Another key parameter in evaluating the material content of components is the pitch of the metallic terminations. The pitch determines the number of contacts per unit length. As the package size increases, the number of contacts also increases, leading to a higher quantity of gold and copper. This trend is confirmed in Fig. 3, which illustrates the gold content as a function of the pin count for various components (more detailed models will be presented in Section 3.1).

In a symbolic representation, a possible vector describing the metal content in PCBs, when considering additional components beyond ICs, can be expressed as:

$$v2 = [v1,\ Al,\ Fe,\ Ni,\ Zn,\ Ta]T$$

The presence of tantalum capacitors on the PCB contributes to the Al, Fe, and Ta content, which are included in the v_2 vector. A detailed analysis of the material composition of tantalum capacitors is provided in Section 3.1.4.

The inclusion of copper, gold, and silver in our analysis is supported by literature. For instance, in (Arshadia et al., 2018), M. Arshadi et al. identify copper as one of the most economically viable base metals for recovery from PCBs. Additionally, the authors recommend conducting a comprehensive study on the precious metal content in various types of electronic waste, emphasizing the high economic value of gold recovery, while noting that the recycling of other metals is comparatively less significant (Arshadia et al., 2018).

W. Van Meensel et al. (Van Meensel et al., 2014) have proposed similar estimation methods, with the key difference that their approach is based on volume calculations, whereas we consider in-plane dimensions.

Each package type listed in this section represents a broad category encompassing all subcategories and variations of the same package. For example, the BGA category includes CBGA (Ceramic BGA), FBGA (Fine BGA), PBGA (Plastic BGA), and others.

In the following sections, we detail the methodology for four specific component types: QFP, BGA, SOIC and tantalum capacitors. Some of the Material Declarations used in this analysis can be found on the following websites: www.analog.com, www.ti.com, www.latticesemi.com, www.xilinx.com, www.altera.com, www.calchipelectronics.com, www.fujicon.com.

Finally, all regression models developed in this study were constructed following a consistent and rigorous methodology, which will not be repeated in the individual model descriptions but is summarized here:

1. Exploratory Analysis: Scatter plots were used to visually assess potential relationships between each independent variable and the corresponding metal content. This initial step supported the selection of candidate predictors.

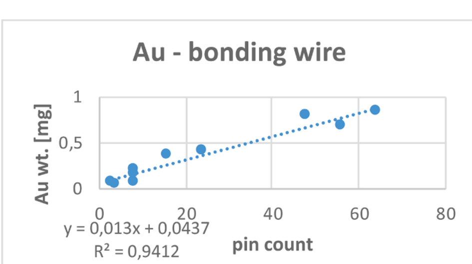

Fig. 3. Gold content (bonding wire) in electronic packages as a function of pin count.

2. Normality Testing: The Anderson-Darling test was applied to both the dependent variable (metal content) and the residuals of the fitted models to verify the normality assumption required for linear regression.
3. Parameter Significance Testing: A two-tailed *t*-test was performed on each regression coefficient, including the constant term, to assess statistical significance. Variables that did not pass the significance test were excluded from the final model to enhance robustness and interpretability.

3.1.1. Analysis of materials in QFP packages

This package belongs to the category of leaded package (with ‘gullwing’ solder joints at the four side of the component). It is a very common package with active electronic functions such as microcontroller, generator, delay buffer, clock, SRAM and more others. It is not uncommon that this package results the biggest on the PCB respect to other small components because it executes the main electronical function analogue to the function executed by the CPU of a motherboard PCB. Since it is often ‘big’, its analysis from a material point of view is very important and not negligible. We propose two models for the estimate of copper and gold content.

3.1.1.1. Model for gold (Au) content. For QFPs with side dimensions smaller than 10.5 mm, an analysis of multiple material declarations suggests using an average gold content of 0.65 mg.

For QFPs larger than 10.5 mm, a regression analysis was conducted to determine the relationship between gold content and pin count. The data used for this regression analysis is presented in Table 2, while Fig. 4 illustrates the gold content [mg] as a function of pin count, revealing a clear linear trend. The final equation obtained is:

$$Au = 0{,}02527 * pin\ count \tag{1}$$

with an R2 = 0963.

Using the data from Table 3, a confidence interval for the linear regression model can also be constructed. When the regression intercept is constrained to pass through the origin, as in this case, the confidence interval is given by the following formula:

$$Y_0 = b_1 x_0 \pm t_{\frac{\alpha}{2},n-1}\sqrt{\frac{SS_r}{n-1}\left(1+\frac{x_0^2}{\sum_t (x_t^2)}\right)} \tag{2}$$

Table 2
Value of gold vs. pin count (QFPs.

Number of contacts	*Gold content [mg]*	*Number of contacts*	*Gold content [mg]*
32	0577	80	1,85
32	0881	80	2,52
44	1093	100	1928
44	1,14	100	2523
48	0999	100	3,41
48	1116	120	1693
48	0974	120	3,9
52	1,03	128	3112
52	1628	128	3104
52	1704	128	2556
52	1006	128	3552
52	1000	128	2354
52	1,42	128	4,16
64	1342	132	5785
64	1147	132	5785
64	1144	144	3407
64	1,09	144	3668
64	1287	144	4524
64	0729	144	3,94
64	1,13	176	4794
80	2449	176	4997
80	2076	176	4,37
80	2114		

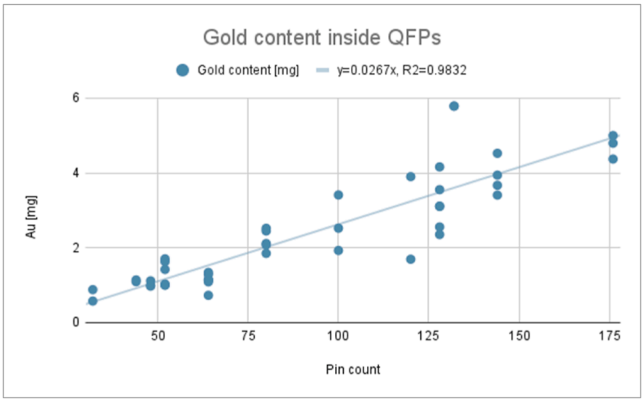

Fig. 4. Regression analysis of gold as a function of the number of contacts (pin count) for QFPs.

Table 3
Percentage error between measured and estimated materials related to Automotive 2 PCB (the error is calculated respect to the total material content value).

Cu Δ measured – estimated [%]	*Cu error %*	*Ag Δ measured – estimated [ppm]*	*Ag error %*	*Au Δ measured – estimated [ppm]*	*Au error %*
0,11	0,0003	251	0,67	4,67	3,81

Where b1 is the estimate for the slope, $SS_r = \sqrt{\sum_{i=1}^{n} (x_i - b_1 x_i)^2}$ and $t_{\frac{\alpha}{2},n-1}$ is the value of the t (Student) statistics with n-1° of freedom at a α/2 confidence level.

Using this formula for Y_0 it is possible to calculate upper and lower confidence intervals (with 95 % of confidence) and superimposing it to the regression analysis. The result is reported in Fig. 5.

3.1.1.2. Model for copper (Cu) content. For QFPs with side dimensions smaller than 10.5 mm, an analysis of multiple material declarations suggests using an average copper content of 47,94 mg.

For QFPs larger than 10.5 mm, a regression analysis was conducted to determine the relationship between copper content and volume. The data used for this regression analysis is presented in Table 4.

The obtained regression is reported in Fig. 6 and in Fig. 7 with confidence intervals. The final equation is:

$$Cu = 0,5212 * volume + 19,484 \tag{3}$$

with an R2 equal to 0,8702.

Note that the package volume can be calculated by knowing the in-plane dimensions and thickness. Similarly, a confidence interval was also determined for the Cu content, with the results presented in Fig. 7.

Table 4
Copper content vs. component volume (QFPs).

Volume [mm^3]	*Copper content [mg]*
81	123,85
279,8432	118,737
113,4	59,09
81	46,392
348,48	55,553
348,48	55,553
144	65,241
144	65,241
81	49,679
144	84,39
201,6	90,202
201,6	76,829
1121,472	705,07
196	109,197
677,6	126,605
677,6	221,306
256	162,577
256	126,577
492,8	812,395
2672,011,249	1414,04
2672,011,249	1414,04
677,6	258,878
3309,696	1640,286
946,4	441,267
946,4	1061,7

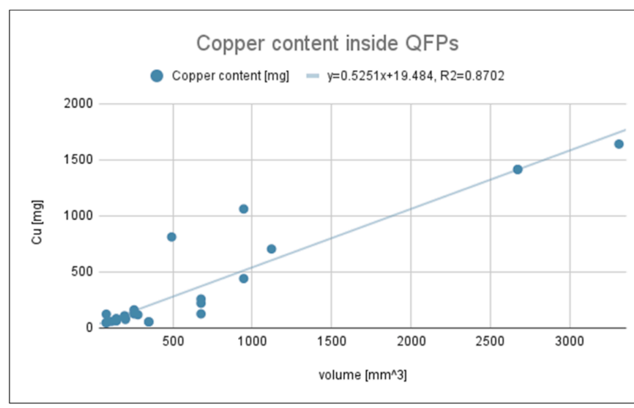

Fig. 6. Regression analysis of copper content as a function of the volume (QFPs.

3.1.2. Analysis of materials in BGA packages

The BGA (Ball Grid Array) is another important SMD (Surface-Mount Device) package. It has a quad-shaped design, with electrical continuity

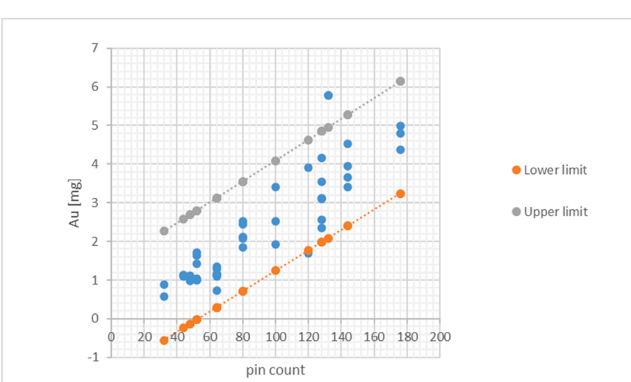

Fig. 5. Confidence interval for gold prevision (QFPs).

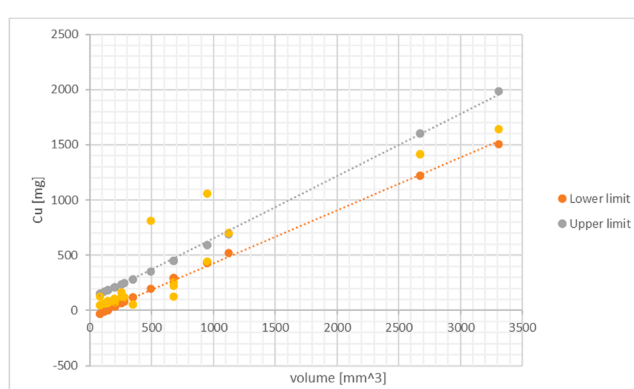

Fig. 7. Confidence interval for copper prevision (QFPs).

to the circuit provided by solder balls made of SAC alloy (typically a SnAgCu eutectic alloy). The side length can reach 30 mm or more, resulting in a significantly higher metal content compared to smaller components.

Unlike QFP (Quad Flat Package), where electrical connections are limited to the four sides, BGA utilizes the entire area beneath the package for electrical connections. As a result, the number of possible electrical connections in a BGA package follows the relation:

$$N \approx (lp) * 2 \tag{4}$$

where l is the side length [mm], and p is the ball pitch [mm].

A key challenge in predicting the material content of BGA packages is that the exact number of solder balls is not easily determined through visual inspection. Additionally, various configurations exist, and not all positions in the quad grid under the package are necessarily occupied by solder balls. Fig. 8 illustrates two different BGA configurations:

a) Full Grid BGA – where all positions are occupied by solder balls.
b) Reduced Grid BGA – where only the four outer rows are used for electrical contacts, along with a smaller internal grid, which may serve either for electrical connections or thermal dissipation.

Between full and reduced configurations there are different hybrid possibilities: in some case, for example, the internal quad is not present. In addition to this, in BGA package the pitch can vary generally from 0,8 to 1,27 mm.

3.1.2.1. Models for gold (Au) content. For BGAs with side dimensions smaller than 7,2 mm, an analysis of multiple material declarations suggests using an average gold content of 0.03 mg.

For BGAs larger than 7,2 mm, a regression analysis was conducted to determine the relationship between gold content and pin count. The data used for this regression analysis is presented in Table 5 and the obtained linear trend is descripted in Fig. 9.

The obtained equation in this case is:

$$Au = 0,6979 * side\ dimension - 4,763 \tag{5}$$

with an R2 equal to 0,97.

Using the number of balls as an independent variable, it is possible to construct the relative statistics in Fig. 10 (linear model) using the data set reported in Table 6.

The obtained equation is:

$$Au = 0,0285 * number\ of\ balls \tag{6}$$

Incidentally, this equation is very similar to the one derived for predicting gold content based on the number of joints in QFPs, which validates the idea of using the package side dimension as the predictor

Table 5
Comparison between predicted and analysed gold content and PCB grade.

PCB labels	*Predicted Au [ppm]*	*Analysed Au [ppm]*	*Predicted grade*	*Analysed grade*
TV	38	58	**Low**	**Low**
Automotive control unit	245	280	**High**	**High**
Network PCB	183	200	**Medium**	**High**
Ram	392	300	**High**	**High**
Motherboard	98	100	**Medium**	**Medium**
Hard disk	265	300	**High**	**High**
DVD reader	163	100	**Medium**	**Medium**

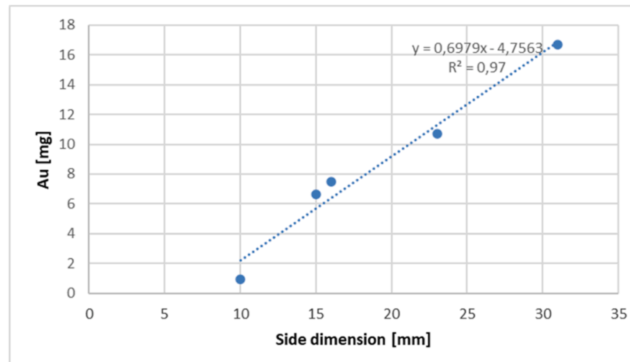

Fig. 9. Regression analysis of gold content vs. the side dimension of the BGA.

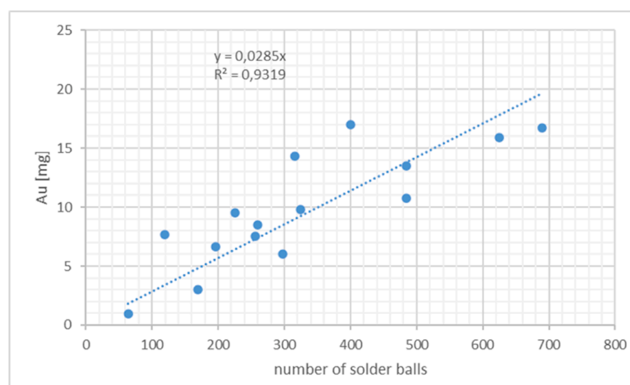

Fig. 10. Regression analysis of gold content as a function of the number of solder balls (BGA).

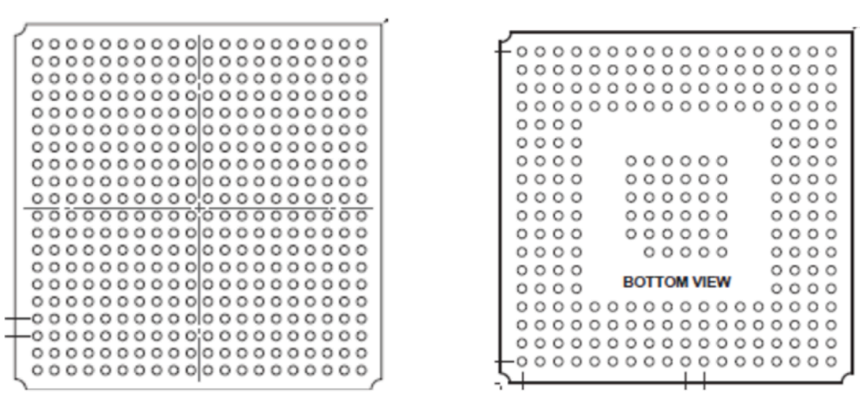

Fig. 8. BGAs full and reduced configurations.

Table 6
Gold content vs. number of solder balls (BGA).

Number of balls	Au content [mg]
64	0956
119	7,66
169	3,03
196	6639
225	9,52
256	7,5
260	8,51
297	6,01
316	14,3
324	9,76
400	17
484	10,728
484	13,5
625	15,9
676	6,69
689	16,7

for the gold content.

3.1.2.2. Models for copper (Cu) content. For BGAs with side dimensions smaller than 12 mm, an analysis of multiple material declarations suggests using an average copper content of 23 mg. For BGAs with dimensions between 12 mm and 16 mm, the same analysis recommends an average quantity of 75 mg.

For BGAs larger than 16 mm, a regression analysis was conducted to determine the relationship between copper content and the dimensions. Based on available data review, the copper mass can be estimated starting from the package mass. For this reason, we first need to have a model to estimate the component mass through the side length. In Fig. 11 the resulting model is shown.

The obtained regression equation is:

$$mass = 173,96 * side - - 1730,2 \tag{7}$$

The predicted mass quickly becomes negative for side dimensions smaller than 10 mm. However, this is not an issue since, for side lengths below 16 mm, a constant average value independent of dimension is used. The dataset variance is sufficiently low, making the inclusion of a confidence interval in the analysis impractical.

To estimate the copper content, a typical percentage can be applied to the predicted mass. An analysis of multiple material declarations suggests using different values depending on the macro sub-category of BGA.:

- For a classic plastic BGA, the typical copper percentage (primarily from the copper frame) is 19 %.
- For other BGA types, such as FPGAs or BGAs with additional copper pads for thermal dissipation, the typical percentage is 28 %.

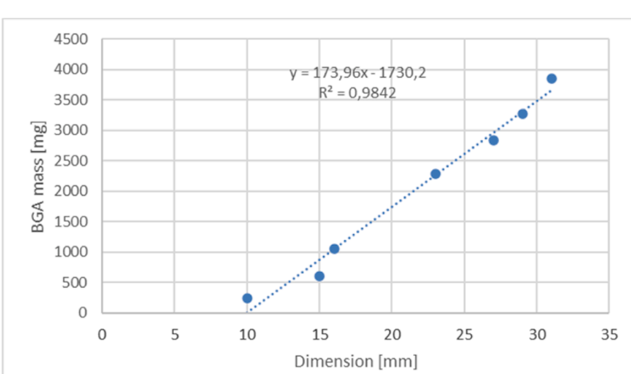

Fig. 11. Weight (mass) of BGA as a function of the side dimension (BGA).

These percentages can be directly applied to the estimated mass to obtain the copper content prediction.

3.1.3. Analysis of materials in SOIC packages

The Small Outline Integrated Circuits, SOICs, packages influence recycling of PCBs for their high frequency on boards, even if they do not contain notable amounts of gold compared to BGA and QFP packages.

3.1.3.1. Model for gold (Au) content. The model has been developed using the number of pins as the sole regressor, given the package design: gold is present exclusively in the bonding wires, which connect each pin to the grid, resulting in one bonding wire per pin.

The data used to develop the model are presented in Table 7.

Data used in the analysis come from 17 different material declarations of packages manufactured by Texas Instruments and Analog.

Result of the regression is a model including only one regressor and no constant:

$$Au = 0,0274 * pin\ count \tag{8}$$

The coefficient of determination (R^2) is 0.833, which is a strong value; however, since the model lacks a constant term, the significance of R^2 is somewhat diminished. Residual analysis confirmed that they are normally distributed and independent.

Although this result appears acceptable, a more detailed data analysis revealed indications for an alternative model. Examining the scatter plot of gold mass versus the number of pins in Fig. 12 suggests the presence of two distinct trends—one with a steeper slope compared to the other.

A deeper investigation showed that these separate trends correspond to two different manufacturers. This finding suggests that the dataset may consist of two subsets with distinct distributions. As a result, separate models were developed for each manufacturer.

Normality tests confirmed that the data for both manufacturers follow a normal distribution. Consequently, a simple linear model—including a constant term and the number of pins as a linear regressor—was fitted for each case.

The resulting model for Texas Instruments packages is:

$$Au = 0,03415 * pin\ count\ - 0,362 \tag{9}$$

In this case, the constant term is retained in the model, with a T-test p-value of 0.021, which is below the predefined significance level. The coefficient of determination (R^2) is 0.8839, indicating an improved fit and greater statistical relevance due to the presence of the constant term. Additionally, residuals were found to be normally distributed, and the runs test confirmed their independence.

The resulting model for Analog packages is:

Table 7
Gold content vs. number of pins (SOIC).

Number of pins	Au content [mg]
8	0.200
8	0.156
8	0.274
14	0.036
14	0.132
14	0.328
16	0.158
16	0.445
16	0.500
18	0.370
18	0.768
20	0.357
20	0.770
24	0.402
24	1.020
28	0.590
28	1.190

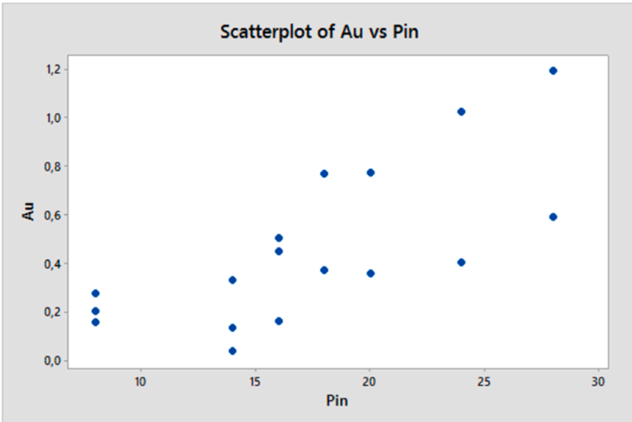

Fig. 12. Gold content versus the number of pins (SOIC).

$$Au = 0,0503 * pin\ count\ - 0,2408 \tag{10}$$

Three different models were fitted to the dataset, each capable of predicting the gold content in SOIC packages. Ultimately, the decision was made to use the two separate models developed for the two manufacturers and to compute the final prediction as the simple average of the results from both models. This approach was chosen to account for the differences between manufacturers, prioritizing two more precise models over a single model with lower statistical significance.

3.1.3.2. Model for copper (Cu) content. The same methodology used to develop the gold prediction model was also applied to analyze the copper mass in SOIC packages. In this, an attempt was made to include the package width in the prediction model, as this dimension could influence the grid area.

T dataset used for the analysis includes packages from three different manufacturers, derived from 19 material declarations. Some declarations correspond to the same package type (in terms of pin count and width) but originate from different manufacturers. The complete dataset is presented in Table 8.

From graphical analysis both width and number of pins seem to be possible regressors for the trend function. A linear regression model has been fitted, and the result is

$$Cu = \ - 82.80 + 10.66 * width\ + 8.01 * pin\ count \tag{10a}$$

The R^2 coefficient is 0.9215 and the adjusted R^2, which accounts for the number of regressors, is 0.9117. These values indicate a good fit of the model.

Table 8
Copper content vs. number of pins and package width (SOIC).

Pin	Copper [mg]	Width [mm]
8	31.7	3.9
8	28.80	3.9
8	26.73	3.9
8	24.87	3.9
14	50.50	3.9
14	97.43	3.9
14	79.55	7.5
16	51.23	3.9
16	95.63	3.9
16	137.00	7.5
16	136.36	7.5
18	133.00	7.5
18	159.47	7.5
20	165.00	7.5
20	145.73	7.5
24	197.00	7.5
24	155.66	7.5
28	215.00	7.5
28	254.53	7.5

3.1.4. Analysis of materials in polymeric capacitors

Polymeric capacitors are the major source of tantalum (Ta) inside PCBs. This kind of component is easily detectable according to two different characteristics: the dark yellow colour and the type of package, the J leaded (the name refers to the shape of the metallic terminations). A typical Polymeric capacitor is depicted in Fig. 13.

To estimate the material content, an average percentage composition is applied to the component weight. Tantalum capacitors, classified under the 'molded components' package type, are available in four different case sizes—labeled A, B, C, and D. Each case size is characterized by an average weight and a typical material composition, as shown in Table 9.

The tantalum content varies between approximately 30 % and 40 % of the total component weight. Each case size has standardized dimensions, as detailed in Fig. 14 and Table 10.

3.1.5. Summary of the prediction models

In the previous sections, we described the internal configuration and material composition of various components, presenting material prediction models for BGAs, QFPs, and SOICs. The modeling efforts were restricted to these component classes for the following reasons:

- *Availability of necessary data for accurate material modeling.* The robustness of the model depends heavily on the quantity and quality of data available from component manufacturers. For example, while it would be theoretically possible to develop a model for electrolytic capacitors—describing the relationship between component mass, cylinder height, and diameter, and then applying typical metal percentages (e.g., Al and Fe) to estimate material composition—this model was not included. The reason is that data on material percentages from a single manufacturer are insufficient to construct a reliable model. To ensure a robust material content prediction, material declarations from multiple manufacturers must be considered.
- *Contribution of specific components to the total material content of the PCB*. Passive components such as ceramic resistors and capacitors are widely used, but their dimensions are significantly smaller than those of integrated circuits (ICs). As a result, their contribution to the overall material content of the PCB is negligible compared to that of larger components.
- *Standardization of components.* Standardization plays a crucial role in modeling. For instance, the approximation methods used for passive ceramic components cannot be directly applied to connectors. Unlike ceramic components, connectors have a non-negligible weight relative to the total PCB weight. However, the wide variety of connector configurations available on the market (as classified in (Charpentier et al., 2024)) makes it difficult to develop a generalized material content model. Additionally, data availability is a challenge, as material declarations for connectors are not as readily accessible as those for ICs, primarily due to strategic and proprietary knowledge constraints.

Finally, regarding the prediction models proposed in paragraphs 3.1.1 (QFP), 3.1.2 (BGA) and 3.1.3 (SOIC), the input data used to model the amount of material are restricted to type of 'package', 'dimensions' and 'pin count'.

Fig. 13. Typical Tantalum capacitor.

Table 9
Typical tantalum content in different case size.

Case A		*Case B*		*Case C*		*Case D*	
Mass [mg]	26	*Mass [mg]*	59	*Mass [mg]*	160	*Mass [mg]*	304
Ag %	3.59	*Ag %*	2.83	*Ag %*	2.61	*Ag %*	2.71
Fe %	9.96	*Fe %*	9.15	*Fe %*	5.73	*Fe %*	4.092
Ni %	7.57	*Ni %*	6.95	*Ni %*	4.35	*Ni %*	3.11
Ta %	31.61	*Ta %*	32.38	*Ta %*	37.19	*Ta %*	41.01

Fig. 14. Tantalum capacitor mechanical drawing.

Table 10
Typical case size for tantalum capacitors.

Case code	*EIA code*	*L*	*W1*	*W2*	*H*	*Z*
P	*2012*	2.0 ± 0.2	1.25 ± 0.2	0.9 ± 0.1	1.1 ± 0.1	0.45 ± 0.1
A	*3216*	3.2 ± 0.2	1.6 ± 0.2	1.2 ± 0.1	1.6 ± 0.2	0.8 ± 0.3
B	*3528*	3.5 ± 0.2	2.8 ± 0.2	2.2 ± 0.1	1.9 ± 0.2	0.8 ± 0.3
C	*6032*	6.0 ± 0.3	3.2 ± 0.3	2.2 ± 0.1	2.5 ± 0.3	1.3 ± 0.3
D	*7343*	7.3 ± 0.3	4.3 ± 0.3	2.4 ± 0.1	2.8 ± 0.3	1.3 ± 0.3
E	*7343*	7.3 ± 0.3	4.3 ± 0.3	2.4 ± 0.1	4.0 ± 0.3	1.3 ± 0.3

On the contrary other data are neglected such as the specific functionality, the manufacturer or the year of production. In the case of ICs, the number of possibilities and combinations are so high that a universal model become a very long and expensive operation to perform. Note that the 95 % confidence intervals provided in Figs. 4 and 6 reflect the variability due manufacturer, functionality and data of production variables.

Fig. 15 represents a practical way of using the models proposed in paragraph 3.1.1, 3.1.2 and 3.1.3. The process begins with a visual inspection of the component to gather basic information: package type, dimensions (both in-plane and out-of-plane, i.e., thickness), and pin count. With this data it is possible to get an estimate of the material content using the models developed in Sections 3.1.1, 3.1.2, and 3.1.3. If this approximation is adequate for the specific end-of-life (EoL) activity, the process concludes successfully. Otherwise, additional data are required. It is not possible to determine 'a priori' whether the approximations are 'good' or 'bad'; this depends on the specific EoL process to be performed (see Section 4.3 for more details).

3.1.6. PCB substrate material and finishing estimate

When the copper on the substrate is not protected by a solder mask, it undergoes a finishing process to prevent oxidation or corrosion during assembly and reflow soldering. The most common finishes include immersion silver, immersion tin, and ENIG (electroless nickel – immersion gold). The typical thicknesses of these finishes are listed in Table 11.

The quantity of material in the finishing can be estimated by multiplying the material density (ρ) by the thickness (s) and the area covered by the finishing (A), as expressed in the following equation:

$$m = \rho * A * s \tag{11}$$

The presence or the absence of extended finishing areas have to be considered in order to evaluate the PCB value.

The copper content in the substrate is given by:

$$m = \rho_{Cu} * \sum_{i=1}^{n} A_i * s_{Cu,i} = \rho_{Cu} * \sum_{i=1}^{n} k_i * A^{tot} * s_{Cu,i} = \rho_{Cu} * A^{tot} * \sum_{i=1}^{n} k_i * s_{Cu,i} \tag{12}$$

It is possible to estimate the quantity of copper in the substrate laminate multiplying the copper density (ρ_{Cu}) times the sum over the number of layers of the copper foil area (A_i) and thickness ($s_{Cu,i}$) for each layer, since copper area and thickness could be different from layer to layer. The copper foil area is in general equal to a fraction of the total PCB area ($k_i * A^{tot}$).

If some data are lacking, approximations can be used. For example, the average value of 35 μm for the cupper foil can be used as s_{Cu}^{approx}. The resulting formula is:

$$m = \rho_{Cu} * A^{tot} * s_{Cu}^{approx} * \sum_{i=1}^{n} k_i \tag{13}$$

We can introduce the average area fraction as $\overline{\boldsymbol{k}} = \frac{\sum_{i=1}^{n} k_i}{n}$, using $\overline{\boldsymbol{k}} =$

Table 11
Typical PCB finishing and thickness.

Finishing material	*Material thickness*
NiAu	Au: 0,1 μm
Ag immersion	Ag: 1 μm
Sn immersion	Sn: 1 μm

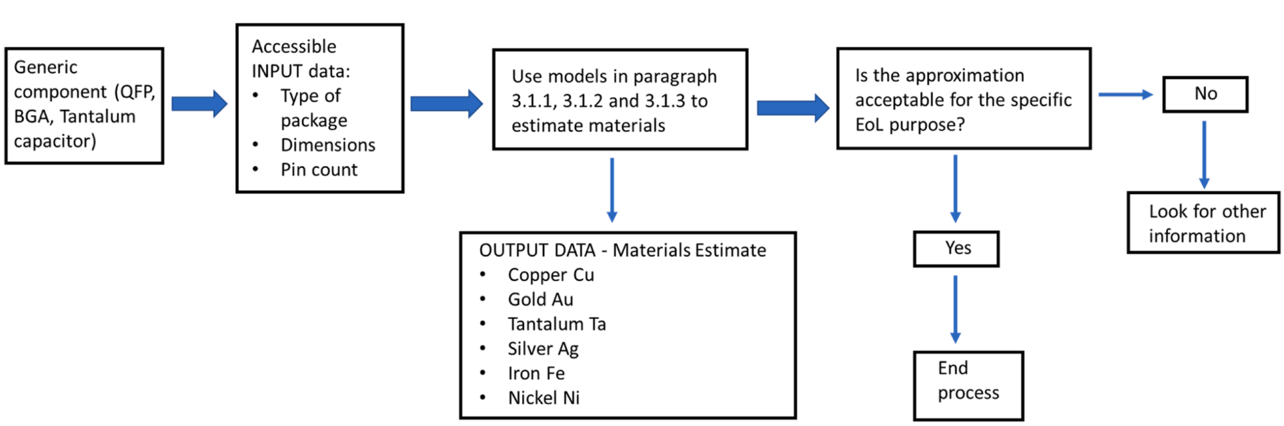

Fig. 15. Flow of steps for the estimate of material content inside QFPs, BGAs and tantalum capacitors.

0.5, and finally approximate the number of layers. Considering the typical commercially available materials, it is possible to construct the Table 12.

For each thickness range, the average of the possible number of layers listed in the third column is used, denoted as n^{approx}. It is important to note that Table 6 presents typical values only; however, as previously mentioned, copper thickness, total PCB thickness, and the number of layers may vary depending on the specific industrial application. For example, in high-performance telecommunication devices, a higher number of layers and copper foil thicknesses smaller than 35 μm are commonly observed. Using these approximations, Eq. (8) simplifies to:

$$m = n^{approx} * \overline{k} * \rho_{Cu} * s_{Cu}^{approx} * A^{tot} \tag{14}$$

Using Eq. (14) rather than (13) depends on the availability of information about the number of layers, copper foil thickness and electronic design of the PC.

3.2. Results and discussion

3.2.1. Comparison between the predicted amount and the chemical analysis

To validate the method presented in this paper we compared the total amount of materials estimated through the models presented in paragraph 3 with the amount of the same materials measured with chemical analysis.

For this purpose, different types of PCBs are considered from different field of application. All SMD standard components are counted and sized with a visual analysis. Table 13 summarizes the electronic packages contained in 'Automotive PCB 1', while Table 14 summarizes the electronic packages in 'Household appliance PCB 1'. Fig. 16 refers to 'Automotive PCB 1' and 'Household appliance PCB 1'.

As a second step, the models presented in paragraph 3 have been used to estimate the materials quantities. Since there are no extended finished surfaces in these PCBs, all the precious metals are inside the components. The total copper amount includes the amount from the copper foil in substrate layers as explained in paragraph 3.2 and the amount from electronic packages as explained in paragraph 3.1. The results are summarized in Table 15.

As a third step, the PCBs have been shredded with a two-step procedure involving both coarse and fine shredder. The fine shredding step have been performed with a 1 mm grid. After this the powders have been removed from the machine and chemically analyzed. The elemental composition of PCBs is detailed in the following tables.

Table 16 compares the calculated and measured gold quantities.

As it can be noticed, the agreement of measured and estimate gold content is very good. According to Umicore classification (see Table 16) 'automotive PCB' is a medium grade PCB and 'household appliance' is a low grade PCB.

Other experiments have been performed to analyze silver (Ag) and copper (Cu) content. Two types of PCBs are considered in the following: 'Automotive PCB 2' and 'Household appliance PCB 2', shown in Fig. 17.

The new electronic packages and materials content are detailed in Tables 17 and 18. In this experiment the analysis in focused on the determination of Cu and Ag content.

The PCBs have been shredded and analyzed with the same procedure used for PCBs 'Automotive 1' and 'Household appliance 1'.

The Table 19 summarizes analysis and compares estimate and measured materials.

Table 12
Typical PCB thickness and numbers of layers.

Thickness range (mm)	*Possible number of layers*	*Average possible number of layers*
0508	4	4
0787 ÷ 1193	4,6	5
1574 ÷ 3175	4,6,8,10	7

Table 13
Number of packages and dimensions related to Automotive PCB 1.

Electronic packages	*Numbers*	*Dimensions [mmxmm]*
QFP	1	32×32 (0,5 mm pitch)
SOT	10	3 × 3
	4	7 × 8
SOIC	1	12×12
	4	5 × 6
	2	7 × 8
	11	2 × 3
J	4	8 × 6
	2	4 × 8
	1	3 × 4
	41	3 × 3

Table 14
Number of packages and dimensions related to Household appliance PCB 1.

Electronic packages	Numbers	Dimensions [mmxmm]
QFP	1	14×14 (0,8 mm pitch)
	1	10×10 (0,8 mm pitch)
SOT	10	3 × 3
	4	7 × 8
D2PK	2	11×6
SOIC	3	5 × 6
	2	7 × 8
J	12	2 × 5
	10	2 × 1

The Cu estimate is reliable, as the Cu analysis is performed using SEM-EDS, which provides only an average measurement within a specific localized area of the powder sample. The same applies to the Ag result, considering that it is based on an ICP semi-quantitative analysis.

3.3. Analysis of the material content value

The predictive methodology is applied to estimate the material content value of the 'Automotive 2' and 'Household Appliance 2' PCBs. As discussed in Section 3.1.4 and shown in Table 4, some approximations are inevitably introduced due to accessibility constraints that limit the availability of input data on the material composition of components. A potential approach to assess the overall impact of these approximations on the accuracy of the method is to analyze the market value of the PCB, considering only its material market value. The value of materials such as gold, silver, and copper fluctuates daily, with gold showing a significant upward trend in recent years. To ensure a representative and current estimation, we used the average market prices for the calendar year 2024, calculated from publicly available monthly price data published by the London Metal Exchange (LME) and LBMA (London Bullion Market Association).

Copper, gold, and silver are the three most critical metals, as their concentrations are highly dependent on the characteristic dimensions of the components (such as package dimensions and the pitch of metallic terminations). By associating each material with its market value (€/kg), the material content value can be determined using Eq. (15).

$$total\ material\ content\ value = \sum_i C_i V_i \tag{15}$$

where Ci is the concentration of the i th material [kg/ton] and Vi is the value of the same material [euro/kg]. In Tables 20 and 21 we list the most important materials related to the experiments previously described and the related value:

The total material content value for PCB 'Automotive 2' is 8802 euro/tons, for PCB 'Household Appliance 1' is 5024 euro/tons.

Applying the same evaluation but restricting it to copper, gold, and silver, the materials that can be predicted through our models, the material content value for PCB 'Automotive 2' is estimated at 8406

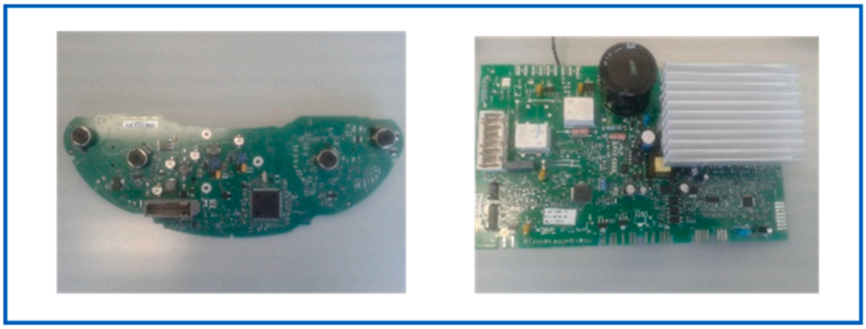

Fig. 16. Automotive PCB 1 and Household appliance PCB 1.

Table 15
Material prediction in PCBs 'Automotive 1' and 'Household appliance 1' based on the developed knowledge-based approach.

PCBs	Cu [mg]	Au[mg]	Ag[mg]
Automotive 1	3474,5	24	53,4
Household appliance 1	2212,5	7,7	17,9

Table 16
Comparison between gold content calculated with extrapolation methods and gold content measured with ICP technique.

PCBs	*PCB Weight [mg]*	*Au[ppm] calculated*	*Au [ppm] Measured (ICP)*
Automotive 1	228,600	105	109,67
Household appliance 1	136,000	57	62,14

€/ton, accounting for 95.5 % of the total value. Similarly, for PCB 'Household Appliance 1,' the material value of copper, gold, and silver represents 94.07 % of the total. This demonstrates that our approach considering only these materials, makes sense if the economic value is the main goal of the PCB grading.

Symbolically, the output of the calculation is represented as the vector v_1 = [Cu Au Ag], which corresponds to the absolute content (in mg) of base and precious metals. By dividing this vector by the PCB weight and applying the necessary unit conversions, the material concentration C [kg/t] can be obtained. Furthermore, if the material content value is expressed as a vector V, where the components represent the market value of Cu, Au, and Ag [€/kg], the approximate material content value of the PCB can be determined using Eq. (16).

$$approx.\ material\ content\ value = \overline{\boldsymbol{C}^T}\boldsymbol{V} = \sum_{i=1}^{3} \overline{C}_i V_i, \tag{16}$$

Table 17
Number of packages and B dimensions related to Automotive PCB 2.

Electronic packages	*Numbers*	*Dimensions [mmxmm]*
QFP	1	32×32 (0.5 mm pitch)
SOT	31	3 × 3
	5	7 × 8
SOIC	1	12×12
	4	5 × 6
J	2	7 × 8
	20	2 × 3
	4	8 × 6

where (Ci) is the estimated concentration.

Another important observation is that only 0.09 % and 0.02 % of the material content value in the 'Automotive' and 'Household Appliance' PCBs, respectively, originates from rare earth elements. The remaining 4.4 % and 5.91 % correspond to other metals, primarily aluminum (Al), iron (Fe), nickel (Ni), and zinc (Zn). These percentages are relatively small, and their market value is negligible compared to that of gold.

It is important to emphasize that this analysis aims to approximate the market value associated with a specific PCB. Therefore, our estimation focuses on the most valuable metals. However, rare earth elements and other metals such as Ni, Al, and Zn remain strategically important from a recycling and resource recovery perspective. This becomes particularly evident given the current scarcity of raw materials—especially rare earth elements—needed for electronic component production. Moreover, as discussed in Sections 1 and 2, the purity of these metals in end-of-life (EoL) PCBs can exceed that of natural ores, further underscoring the strategic significance of recovering these materials from electronic waste.

The error in the estimated versus measured material content value for Cu, Au, and Ag is analyzed in the following section. This error can be determined using Tables 17 and 18 for the total material content value and Tables 12 and 15 for the discrepancies between measured and

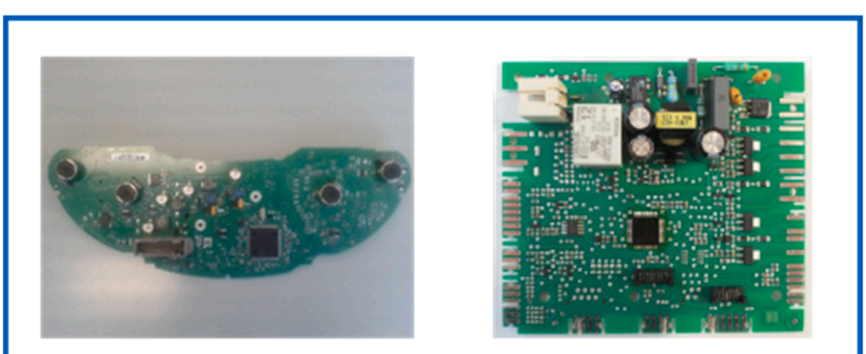

Fig. 17. Automotive PCB 2 and Household appliance PCB 2.

Table 18
Number of packages and dimensions related to Household appliance PCB 2.

Electronic packages	*Numbers*	*Dimensions [mmxmm]*
QFP	1	13×13 (0,6 mm pitch)
SOT	17	3 × 3
	4	7 × 8
D2PK	1	10×6
SOIC	1	9 × 9
J	3	2 × 1

Table 19
Comparison between copper and silver content calculated with extrapolation methods and copper and silver content measured with SEM-EDS and ICP semi-quantitative techniques.

PCBs	*PCB Weight [mg]*	*Cu [%] calculated*	*Ag[ppm] calculated*	*Cu [%] Measured (SEM-EDS)*	*Ag [ppm] Measured (ICP semi-quantitative)*
Automotive PCB 2	137,000	2,25	486	2,36	235,1
Household appliance PCB 1	131,000	1,68	136	1,87	255,6
Household appliance PCB 2	46,000	3,21	226	2,22	237,2

estimated values. Since PCBs 'Automotive 1' and 'Automotive 2' exhibit very similar characteristics, the same approach applies to both. The error can be calculated using the following equation, where the symbols are consistent with those in Eqs. (15) and (16):

$$error_i\% = 100 * \frac{(C_i - \overline{C}_i) * V_i}{total\ material\ content\ value} \tag{17}$$

The results are summarized in Tables 3 and 22.

As observed, the percentage error is higher for precious metals compared to copper, primarily due to the significantly higher market value of precious metals. It is important to note that the total material content value is calculated using Ci, which represents the measured material concentration. The error in material content value is below 5 % for copper, silver, and gold in PCB Automotive 2, while in PCB Household Appliances 1, the error reaches 9.6 %.

Table 20
Material content value of Automotive 2 PCB.

Automotive 2 PCB	*ppm*	*Kg/ton*	*euro/kg*	*euro/ton*
Au	109,67	0,10,967	*71,782*	7872,332
Pd	10,53	0,01,053	*32,072*	337,718
Ce	7,63	0,00,763	*855*	6524
La	3,68	0,00,368	*1662*	0006
Y	18	0018	*1758*	0032
Dy	12,51	0,01,251	*3,23*	0040
Nd	2,97	0,00,297	*294,5*	0875
Pr	0,73	0,00,073	*71,25*	0052
Eu	1,56	0,00,156	*85,5*	0133
Gd	0,69	0,00,069	*342*	0236
W	2,88	0,00,288	*32,3*	0093
Mo	3,2	0,0032	*31,35*	0100
Ag	235	0235	*44,65*	10,493
Mg	1	10	*2755*	27,550
Al	2,89	28,9	*2185*	63,147
Fe	1,02	10,2	*0105*	1071
Ni	0,2	2	*16,625*	33,250
Cu	2,36	23,6	*8,36*	197,296
Zn	0,27	2,7	*2565*	6926
Sn	0,75	7,5	*28,5*	213,750
Sb	0,24	2,4	*12,825*	30,780
Total				8802,403

Table 21
Material content value of Household appliance 1 PCB.

Household appliance 1 PCB	*ppm*	*Kg/ton*	*euro/kg*	*euro/ton*
Au	62,14	0,06,214	30,630	4460,53
Pd	3,44	0,00,344	17,010	110,33
Ce	8,86	0,00,886	9,2	0,01
La	14,7	0,0147	9,2	0,03
Nd	5,85	0,00,585	80	0,42
Pr	1,55	0,00,155	162	0,13
Eu	1,27	0,00,127	628	0,43
Gd	0,73	0,00,073	88	0,02
W	2,96	0,00,296	0,3	0,09
Mo	2,7	0,0027	17,67	0,12
Ag	255,6	0,2556	500	218,54
Mg	0,32	3,2	2,11	8,82
Al	2,54	25,4	2	55,50
Fe	0,81	8,1	0,6	0,85
Ni	0,02	0,2	13,6	3,33
Cu	1,87	18,7	6,2	156,33
Zn	0,37	3,7	1,88	9,49
Total				5024,97

These findings indicate that the proposed method is effective in classifying PCBs based on material value. Given that approximately 90 % of the total material content value is derived from copper, silver, and gold, and that the error in material value estimation relative to the total PCB material content remains within 5–7 % for each analyzed material, the method proves to be a reliable tool for PCB classification.

3.4. Determination of the PCB grade for sorting purposes

The analysis of the market value of precious metals in PCBs, presented in the previous section, aimed to strengthen the predictive method by incorporating economic considerations. However, a key limitation of that initial analysis was its scope, which included only two application domains: automotive and household appliances. As shown in Tables 19 and 20, the discrepancy between the estimated and measured gold concentration (ppm) is relatively small in this case, allowing to expect the models to be reliable. But does this hold true for other PCB categories?

Before addressing this question through additional analyses, it is useful to refer to Fig. 13, which outlines the steps of the proposed method. The central question posed in this figure is: "Is the approximation acceptable for the specific EoL purpose?" But what exactly do we mean by EoL purpose? If a highly precise material content estimation is required, the input data used in this analysis may be insufficient (as discussed in Section 4.2), and additional information may be necessary to improve the accuracy of the estimate. On the other hand, if the goal is a general classification of PCBs for sorting purposes based on material content value, then the proposed models are effective.

To assess the broader applicability of the method, the analysis has been extended to seven distinct PCB categories: TV, automotive control unit, network, RAM, motherboard, hard disk, and DVD reader. These categories cover a diverse range of end-use applications and PCB architectures. Fig. 16 shows examples of these boards, while Table 5 summarizes the comparison between predicted and chemically measured gold content using inductively coupled plasma (ICP) analysis.

The material quantities for these PCBs were estimated using the

Table 22
Percentage error between measured and estimated materials related to Household appliance 1 PCB (the error is calculated respect to the total material content value).

Cu Δ measured – estimated [%]	*Cu error %*	*Ag Δ measured – estimated [ppm]*	*Ag error %*	*Au Δ measured – estimated [ppm]*	*Au error %*
0,19	0,0007	119,6	2,04	5,14	7,34

methods described in Section 3. It is important to note that while Fig. 18 depicts only one PCB per category, both the estimation method and the chemical analysis (ICP) consider multiple subcategories within each macro-category. For example, the RAM category includes four different subcategories, as illustrated in Fig. 19.

PCBs have been shredded and the gold content is the output of the chemical ICP analysis.

The values in Table 5 clearly show that the method developed in this study is effective in predicting the grade of PCBs based on estimated gold content. Out of the seven evaluated cases, the model accurately classified six boards into the correct grade category, corresponding to an 86 % grade prediction accuracy. While the precise gold concentration estimation may be subject to some uncertainty due to the approximations described in Section 3.1.4, the differences remain within an acceptable range for the intended purpose.

To provide a more quantitative assessment of prediction accuracy, three widely used error metrics were calculated: the Mean Absolute Error (MAE) is 37.71 ppm, the Root Mean Squared Error (RMSE) is 47.17 ppm, and the Mean Absolute Percentage Error (MAPE) is 23.3 %. While a MAPE of ~23 % indicates a moderate level of deviation when estimating exact concentrations, it remains sufficiently accurate for grade classification tasks, where precise chemical quantification is not required. In particular, the MAE of 30.3 ppm represents a small absolute deviation relative to typical gold concentration ranges found in PCBs—from ~50 ppm (low-grade) to over 400 ppm (high-grade).

The higher RMSE compared to MAE suggests some variation due to outliers (e.g., RAM and DVD reader), but this does not significantly affect the overall performance of the model in its primary application.

To further illustrate the accuracy of the predictive model, Fig. 20 presents a comparison between the predicted and chemically analyzed gold content. The scatter plot demonstrates a strong alignment between predicted and actual values, particularly for high- and medium-value boards, which are the most critical for grading. Most data points lie close to the identity line, indicating reliable estimation performance. This visual evidence complements the statistical metrics, which report a Mean Absolute Error (MAE) of 37.71 ppm, Root Mean Squared Error (RMSE) of 47.17 ppm, and a Mean Absolute Percentage Error (MAPE) of 23.3 %, confirming the robustness of the model for material value prediction and grade classification.

Finally, a full Bland-Altman analysis is outside the current scope but will be considered in future work to better quantify agreement at the level of measurement bias.

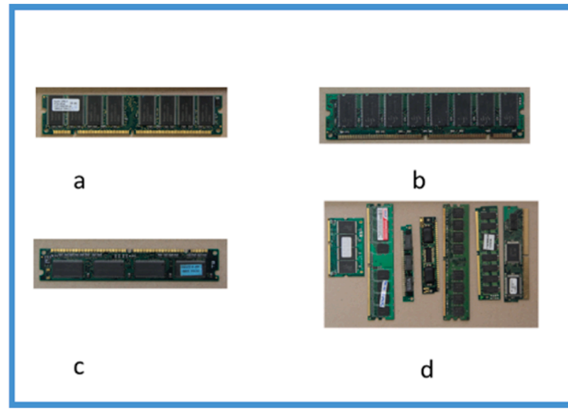

Fig. 19. RAM sub-categories: with ICs (SOICs) on top side(a) with ICs (SOICs) on both top and bottom side (b) with 4 ICs (SOICs) (c) Mix-type RAMs (d).

It is worth emphasizing that the objective of this method is not detailed chemical analysis, but rather a rapid, low-cost, and visual-based estimation of PCB value to support automated sorting decisions in recycling operations. It is important to emphasize the end-of-life (EoL) purpose of the model: when high-precision estimates are needed for regulatory or financial reporting, the current input data may be insufficient and additional compositional analysis would be necessary (see Section 4.2). However, when the goal is efficient value-based sorting, the level of approximation provided by the proposed method is both practical and effective.

4. Conclusions

This paper presents a novel, geometry-based method for estimating the material content of waste PCBs using a knowledge-driven classification of electronic components. By analyzing geometric and functional features—such as the number, size, and type of surface-mounted components—the method estimates the content of valuable metals, particularly gold (Au), silver (Ag), and copper (Cu), which together account for approximately 90 % of the total economic value of most PCBs.

The method was validated on a representative sample of real-world PCB types. Although there is inherent variability in the predicted

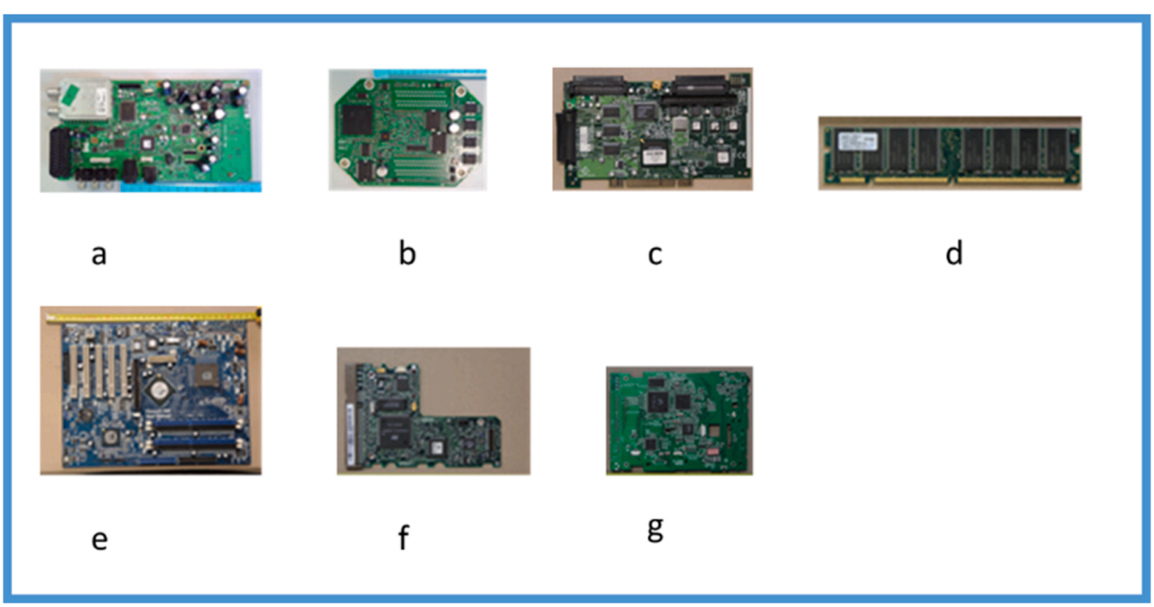

Fig. 18. End of Life PCBs used for grade determination TV (a) Automotive control unit(b) Network(c) RAM(d) Motherboard(e) Hard Disc(f) DVD Reader (g).

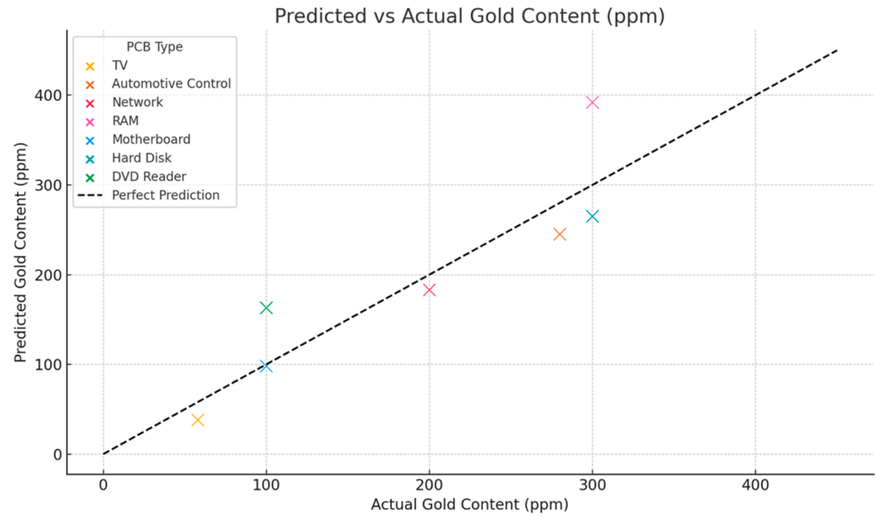

Fig. 20. Scatter plot comparing predicted vs. actual gold content (in ppm) for each PCB type.

metal quantities, the model demonstrated strong practical performance: it achieved high accuracy in predicting PCB grade classifications for the analysed samples, which are primarily determined by gold content. Quantitatively, the model yielded a Mean Absolute Error (MAE) of 37.7 ppm and a Mean Absolute Percentage Error (MAPE) of 23.3 % in gold content estimation. These results indicate that the approach is sufficiently accurate for value-based classification and sorting, especially in SME contexts where high-cost chemical or spectroscopic analysis is not feasible.

However, some limitations remain. The accuracy of the predictions depends on the visibility and correct identification of components on the PCB surface. Boards with non-standard component layouts or densely packed elements may yield higher estimation errors. Additionally, the current method relies on a material database populated with average composition values for each component type, which may not fully reflect manufacturer-specific variations in design or materials.

Future work could address these limitations by enhancing the classification system with AI-based visual recognition, enabling more robust and scalable identification of components under variable conditions. Expanding the material database through broader sampling of PCB types and brands would also improve prediction fidelity. Finally, integrating this method with robotic disassembly systems and real-time imaging hardware could enable fully automated, in-line PCB grading and sorting, contributing to a more efficient and economically viable e-waste recycling process.

During the preparation of this work the author(s) used ChatGPT in order improve the writing clarity. After using this tool/service, the author(s) reviewed and edited the content as needed and take(s) full responsibility for the content of the publication.

CRediT authorship contribution statement

Paolo Citterio: Writing – review & editing, Formal analysis. **Francesco Baiguera:** Writing – original draft, Validation, Methodology, Formal analysis. **Marcello Colledani:** Validation, Supervision.

Declaration of competing interest

The authors declare that they have no known competing financial interests or personal relationships that could have appeared to influence the work reported in this paper.

Data availability

The authors are unable or have chosen not to specify which data has been used.

References

Arshadia, M., Yaghmaeia, S., Mousavib, S.M., 2018. Content evaluation of different waste PCBs to enhance basic metals recycling. Resources, Conservation & Recycling 139, 298–306.
Charpentier, Nicolas M, Xia, Dong, Gabriel, Jean-Christophe P, 2024. Printed circuit board recycling: avfocus on a novel, efficient and sustainable process for spent critical metals recovery. Comptes Rendus. Chimie, 27 (S4), 1–11.
Colledani, Marcello, Copani, Giacomo, Tolio, Tullio, 2014. De-Manufacturing Systems. Procedia CIRP 17 (14 –19).
Cui, Jirang, Forssberg, Eric, 2003. Mechanical recycling of waste electric and electronic equipment: a review. J. Hazard. Mater. B99 (243–263).
Delfini, M., Ferrini, M., Manni, A., Massacci, P., Piga, L., Scoppettuolo, A., 2011. Optimization of precious metal recovery from waste electrical and Electronic Equipment boards. J. Environ. Prot. (Irvine, Calif) 2, 675–682.
Goleva, Artem, Cordera, Glen D., Rhamdhani, M.Akbar, 2019. Estimating flows and metal recovery values of waste printed circuit boards in Australian e-waste. Miner. Eng. 137, 171–176.
Guarde, D., Egia, A., Sánchez, J.C., 2014. Technologies for pre-treatment, disconnection and sorting under development within reclaim project. In: Going Green – CARE INNOVATION 2014 conference.
Havlik, T., Orac, D., Berwanger, M., Maul, A., 2014. The effect of mechanical–physical pretreatment on hydrometallurgical extraction of copper and tin in residue from printed circuit boards from used consumer equipment. Miner. Eng. 65, 163–171.
Kasper, A.C., Berselli, G.B.T., Freitas, B.D., Tenório, J.A.S., Bernardes, A.M., Veit, H.M., 2011. Printed wiring boards for mobile phones: characterization and recycling of copper. Waste Manag. 31, 2536–2545.
Kaya, Muammer, 2016. Recovery of metals and nonmetals from electronic waste by physical and chemical recycling processes. Waste Manag. 57 (64–90).
Kleber, F., Pramerdorfer, C., Kampel1, M., Comanesco, B., Stanciu, E., 2014. Chemical analysis and Computer vision based recognition of electronics waste. In: Going Green – CARE INNOVATION 2014 conference.
Lee, J., Kim, Y., Lee, J.-C., 2012. Disassembly and physical separation of electric/ electronic components layered in printed circuit boards (PCB). J. Hazard. Mater. 241–242, 387–394.
Li, J., Shrivastava, P., Gao, Z., Zhang, H.-C., 2004. Printed circuit board recycling: a State-of-the-art survey. IEEE Trans. Electron. Packag. Manuf. 27 (1).
Marques, André Canal, Cabrera, José-María, Malfatti, Célia de Fraga, 2013. Printed circuit boards: a review on the perspective of sustainability. J. Environ. Manage. 131 (298–306).
Park, Young Jun, Fray, Derek J., 2009. Recovery of high purity precious metals from printed circuit boards. J. Hazard. Mater. 164 (1152–1158).
Park, Seungsoo, Kim, Seongmin, Han, Seongsoo, Kim, Boram, Kim, Byeongwoo, Han, Yosep, Park, Jaikoo, 2018. Liberation characteristics assessment for copper component in PCB comminution product by image analysis. Mater. Trans. 59 (9), 1493 to 1500. 2018.
Pramerdorfer, Christopher, Kampel, Martin, 2015. A dataset for computer-vision-based PCB analysis. In: 14th IAPR International Conference on Machine Vision Applications (MVA) May 18-22. Miraikan, Tokyo, Japan.

Soomro, Iftikhar A., Ahmad, Anser, Raza, Rana H., February 2022. Printed circuit board identification using deep convolutional neural networks to facilitate recycling. Resources, Conservation and Recycling Volume 177.

Tolio, Tullio, Bernard, Alain, Colledani, Marcello, Kara, Sami, Seliger, Guenther, Duflou, Joost, Battaia, Olga, Takata, Shozo, 2017. Design, management and control of demanufacturing and remanufacturing systems. CIRP Annals 66 (2), 585–609. ISSN 0007-8506.

Van Meensel, W., Willems, G., Cauwe, M., 2014. Material identification in electronics. In: Going Green – CARE INNOVATION 2014 conference.

Vetri Murugan, R., Bharat, S., Deshpande, Abhijit P., Varughese, Susy, Haridoss, Prathap, 2008. Milling and separation of the multi-component printed circuit board materials and the analysis of elutriation based on a single particle model. Powder Technol. 183 (169–176).

Wang, X., Gaustad, G., 2012. Prioritizing material recovery for end-of-life printed circuit boards. Waste Manag. 32, 1903–1913.

Yamane, L.H., de Moraes, V.T., Espinosa, D.C.R., Tenório, J.A.S., 2011. Recycling of WEEE: characterization of spent printed circuit boards from mobile phones and computers. Waste Manag. 31, 2553–2558.

de Carvalho, Maria Cristiane Neves, de Souza, Ana Paula Silva, de Oliveira Neto, José Francisco, Silva, Maisa Mendonça, Florencio, Lourdinha, Santos, Simone Machado, February 2025. Management and recovery of critical and strategic raw materials from E-Waste: a case study in Brazil with a focus on printed circuit boards. J. Hazardous Mater. Adv. Vol. 17.